Demonstration of Range & Doppler Compensated Holographic Ladar

Jason Stafford[a], Piotr Kondratko[b], Brian Krause[b], Benjamin Dapore[a], Nathan Seldomridge[b], Paul Suni[b], David Rabb[a]

(a) Air Force Research Laboratory Sensors Directorate
(b) Lockheed Martin Coherent Technologies

Abstract: Holographic ladar systems rely on the capture of temporally stable optical fringe patterns resulting from interference between the local oscillator (LO) beam and signal light imaged from a target. For pulsed systems, fringe visibility is maximized when the LO is temporally matched with the arrival time and duration of the signal, and when there is no gross relative motion between the sensor and target. In this demonstration, both range and velocity of a moving target were measured with a co-aligned high pulse rate laser range finder. Temporal matching was achieved by pulsing the LO to overlap the range-dependent signal arrival. Gross Doppler was compensated by using an acousto-optic modulator to impose a frequency shift onto the LO and transmitter (TX) that corresponded to the measured velocity. Range offset was compensated from ~200 m to >700 m and Doppler compensation was demonstrated from stand-still to full speed of the test vehicle (~24 m/s).

Keywords: Range and Doppler compensation, digital holography, holographic imaging, coherent ladar

1. Introduction

Holographic ladar systems rely on the capture of temporally stable optical fringe patterns resulting from interference between the local oscillator (LO) beam and signal light imaged from a target. For pulsed systems, fringe visibility is maximized when the LO is temporally matched with the arrival time and duration of the signal, and when there is no gross relative motion between the sensor and target. Temporal mismatching causes system efficiency degradation as the entire signal duration is not mixed with the LO beam. Additional degradation is caused by the fact that the LO is producing shot-noise on the camera during signal duration. Relative system to target motion, such as reflecting light off a moving target, causes temporal motion of the fringe phase. Unless compensated this effect again causes reduction of fringe visibility over the pulse duration. This work demonstrates a digital holography system that compensated for both effects of temporal signal to LO alignment and relative Doppler motion.

Both range and velocity are measured with a co-aligned high pulse rate laser range finder. Range data is captured directly, while velocity is calculated as range-rate, i.e. the rate at which the range is changing over time. Temporal matching can then be achieved by calculating the range-dependent arrival time of signal photons and ensuring the LO is on only when the signal is present at the receiver. Gross Doppler compensation is achieved by filtering and estimating velocity and imposing equivalent Doppler frequency shifts into a tunable acousto-optic modulators on the LO and TX light paths.

2. Theory and Performance Predictions

The system efficiency η in the presence of temporal mismatch (τ) or Doppler frequencies f_D can be calculated from the cross-ambiguity function $X(\tau,f_D)$ as $\eta = |X(\tau, f_D)|^2$, where $X(\tau, f_D) = \int_{-\infty}^{\infty} E_S(t)E_{LO}^*(t-\tau)e^{i2\pi f_D t}\,dt$. $E_S(t)$ and $E_{LO}(t)$ correspond to the normalized electric field at time t of the signal and LO beams, respectively. In the case of a unity amplitude rectangular signal of duration t_p mixing with an identical LO pulse, with no Doppler shift, this reduces to $\eta = \left[1 - \left(\tau/t_p\right)\right]$, i.e. an efficiency loss

linear with time offset. In coherent detection scenarios the effective loss is somewhat higher as the receiver integrates shot noise even during the non-overlapped time.

Similarly, in the case of temporally matched pulses in the presence of a Doppler shift the efficiency takes the form $\eta = \mathrm{sinc}^2(f_D t_p)$.

When the pulse duration is short compared with a Doppler cycle the efficiency loss is low. When the pulse duration equals a full Doppler cycle the efficiency is zero; physically this means that the first half of the pulse integrates positive contributions while the second half integrates negative contributions due to the sign change of the coherent mixing, leading to a complete cancellation of the positive contribution.

Radiometric calculations were conducted using the following key design parameters listed in Table 1.

Table 1: Key Design Parameters

Parameter	Value
Transmitted peak power (P)	114 mW
Wavelength (λ)	1545 nm
Pulse width (t_p)	300 ns
Illuminated spot diameter on target (2ω)	30 cm
Target reflectivity (ρ/Ω)	64 sr^{-1}
System efficiency (η)	35%
One-way atmospheric transmission (T)	96%

Predicted CNR was estimated from the equation

$$CNR = \eta \frac{\lambda^3}{hc} T^2 \left(\frac{\rho}{\Omega}\right) \frac{P t_p}{\pi \omega^2}. \quad (1)$$

Implicit in the calculations is that $C_n^2 < 9.3.10^{-13}\ m^{-2/3}$ in order to maintain a ~30 cm illumination spot diameter at the target. The system was estimated to achieve CNR spanning 8 to 24 dB depending on selected target reflectivity and by choosing pulse duration between 100 and 300 ns pulse width.

3. Experiment

Figure 1 illustrates the proposed layout of the DH optical system. Key hardware components are an 11" Celestron telescope, and a FLIR SC2500 320x256 pixel InGaAs camera.

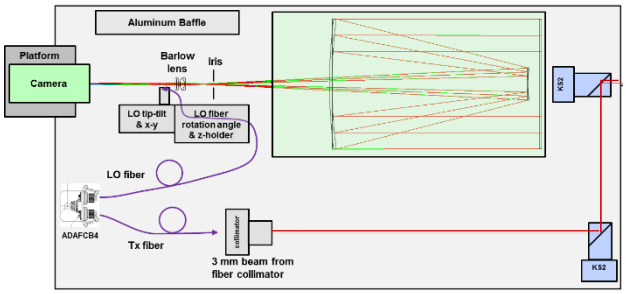

Figure 1. Physical layout of designed system on a 24" x 48" optical breadboard

Figure 2 shows the functional diagram of the source and control system as was implemented. The transmit portion begins with a CW seed laser, which is pre-amplified and split into two paths using a polarization maintaining (PM) 50/50 fiber splitter. Following the splitter, the bottom leg in the figure becomes the LO path while the upper leg becomes the target illumination leg (TX). The two paths are routed through their respective acousto-optic frequency shifters (AOFS). These components adjust the frequency of the input light according to the measured target Doppler. Each AOFS is operated at 200 MHz center frequency at zero Doppler and is capable of ±50 MHz frequency shift. The amount of shift is controlled by a CW voltage

that originates from software driven PXI controller with analog output (AO) voltage. Due to the dual frequency shifter implementation (on LO and TX legs), the determined target Doppler is evenly divided

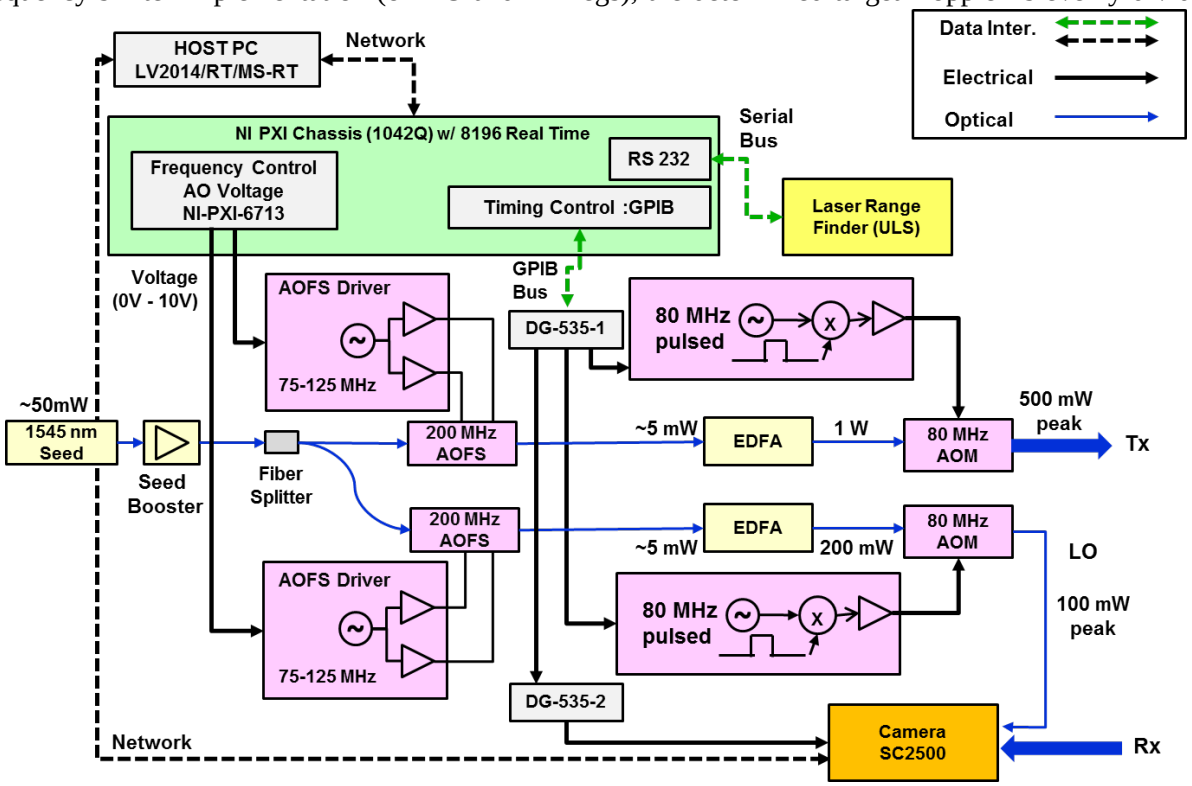

between the LO and TX AOMs.

Figure 2: Functional diagram of range and Doppler compensation system

Following the Doppler-compensation AOMs, the two paths are amplified with respective erbium doped fiber amplifier (EDFA). Each leg following the EDFA has a fixed frequency (80 MHz) AOM that carves out pulses from the CW laser beams. The pulse carving must be performed after the CW amplifiers to prevent possible damage to the EDFAs.

Timing of the fixed frequency AOMs is achieved by control system commanded by the DG535 digital delay generator. This enables correct alignment of the delay of the LO pulse relative to the TX pulse in order to ensure temporal overlap of the two signals. The timing control circuit also triggers the camera to capture digital holography data in synchronicity with the return signal.

The laser range finder, through a serial interface, reports target range and intensity information to the real-time controller. A host computer that interfaced to the real-time controller using a standard network interface served as a graphical user interface with control, data monitoring, and data logging.

The real-time controller was designed to perform three time critical tasks: acquire range, calculate Doppler, and estimate the movement of the target. The state-machine architecture included a thread that received the velocity data and calculated the frequency offsets for the LO and TX optical paths. In addition, it used a Kalman filter to improve the real-time performance of the compensation.

4. Test Results

The field campaign consisted of static and moving target acquisitions. The test scenarios included driving a car at approximately 5, 10, 13, 16, and 24 m/s. The test also included non-moving target data collection at various fixed ranges. The system performance results are plotted in Figure 3.

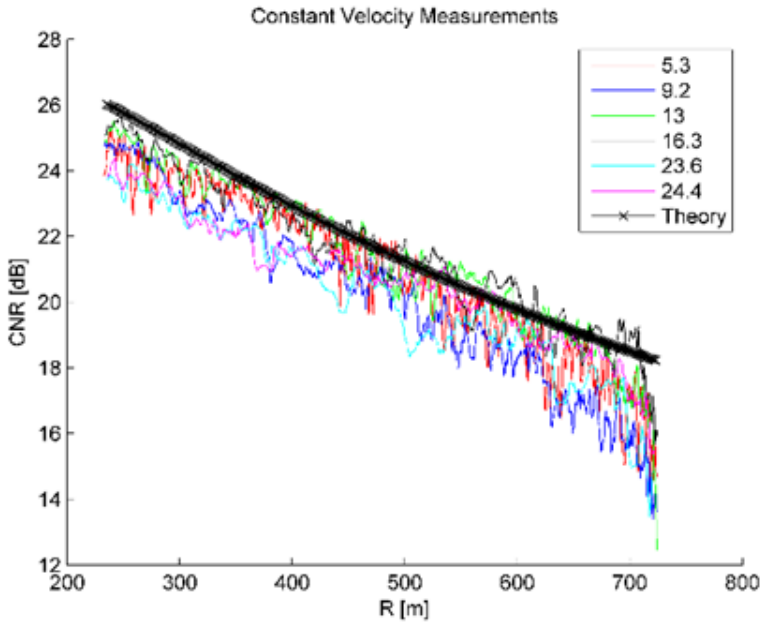

Figure 3. CNR vs. range for moving and non-moving target

The theory line of Fig. 3 includes the output of Eq. 1 as well as numerical modeled effects of the sensor modulation transfer function and physical optics effects such as range dependent vignetting. No visible evidence of CNR loss due to range and Doppler ambiguity was observed when comparing the static to moving target.

A rectangular LO and signal pulse filter overlap efficiency function is evaluated to be

$$\eta_z(f_d, t_d) = \frac{T^2}{T_u T_v} sinc^2(f_d T), \tag{2}$$

where

$$T = \begin{cases} T_v & t_d \le (T_u - T_v)/2 \\ (T_u - T_v)/2 - t_d & \frac{T_u - T_v}{2} < t_d \le (T_u - T_v)/2. \\ 0 & (T_u - T_v)/2 < t_d \end{cases} \tag{3}$$

T_u and T_v are the LO and signal rectangular pulse widths, respectively, and t_d and f_d are the time and frequency parameters tailored by range and Doppler offsets. The efficiency solution assumes $T_u \ge T_v$ and for the reason that the theory is reciprocal in u and v, a symmetric expression applies when $T_v \ge T_u$. This function is maximized when $T_u = T_v$ and this specific condition was implemented for the range and Doppler ambiguity measurement.

A final system demonstration consisted of mapping-out the system range and Doppler ambiguity function for a stationary target by sweeping the pulse and Doppler offsets using the software of the tracking system. The range offset was swept from -350 ns to 350 ns at 25 ns interval while the velocity offset was swept from -5 m/s to 5 m/s at 0.2 m/s interval.

Figure 4 shows the measured range and Doppler ambiguity function where residual gross range offset is evident. This is due to uncompensated physical parameters of the system such as mismatched optical path lengths in the separate LO and TX legs. For comparison, the theoretical model adapted from Eq. (2) is presented in the right of Figure 4. The theory includes an exponential rise/fall time based on the AOM model used in the experiment. The experiment amplitude dependence on range and Doppler offset shows good similarity with the model.

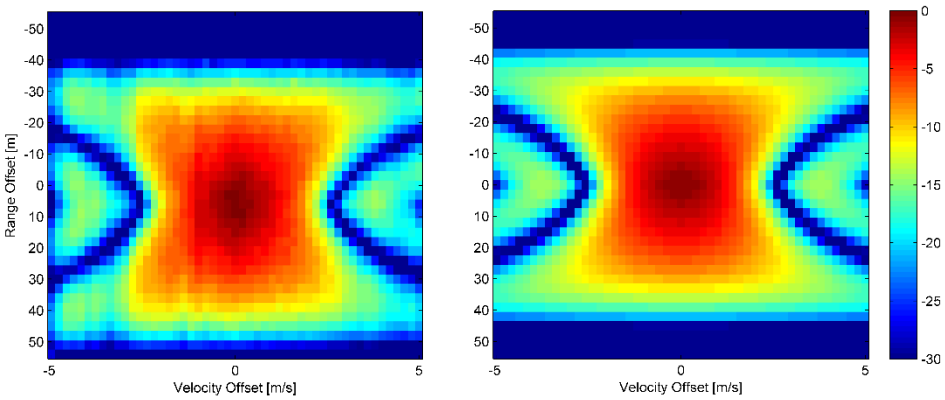

Figure 4. (left) Measured CNR vs. range and Doppler offset. (right) Theoretical CNR vs. range and Doppler offset obtained from Eq. (4). CNR is displayed in dBs.

5. Conclusion

This work summarized the hardware design, system implementation, and demonstration of range and Doppler compensation subsystem to be used with a holographic ladar system built at AFRL. The primary objective of the program was to support AFRL/RYMM with a demonstration that frequency shifting and pulse range positioning technique could be used to compensate for range and Doppler effects while a target mounted to a vehicle was driven down the runway at Wright-Patterson AFB in Dayton, OH. LMCT developed and delivered the software, and participated in field tests of the developed system. The field demonstrations showed that range could be compensated from ~200 m to >700 m and that Doppler compensation was feasible from stand-still to full speed of the test vehicle (~24 m/s).

Future work includes range and Doppler compensation subsystem development for multiple receiver and multiple transmitter digital holography systems operating from ground and air platforms.

The team is also grateful for additional system analysis from John Novotny at LMCT and for logistics and field support from Steve Erisman, Dirk Adams, Bruce Smotherman (Leidos) and Jeff Widiker (MZA) at WPAFB.